

# Control of scroll wave turbulence using resonant perturbations

S. W. Morgan, I. V. Biktasheva, and V. N. Biktashev

*Department of Mathematical Sciences, University of Liverpool, Liverpool L69 7ZL, UK and*

*Department of Computer Science, University of Liverpool, Liverpool L69 3BX, UK*

(Dated: October 24, 2018)

Turbulence of scroll waves is a sort of spatio-temporal chaos that exists in three-dimensional excitable media. Cardiac tissue and the Belousov-Zhabotinsky reaction are examples of such media. In cardiac tissue, chaotic behaviour is believed to underlie fibrillation which, without intervention, precedes cardiac death. In this study we investigate suppression of the turbulence using stimulation of two different types, “modulation of excitability” and “extra transmembrane current”. With cardiac defibrillation in mind, we used a single pulse as well as repetitive extra current with both constant and feedback controlled frequency. We show that turbulence can be terminated using either a resonant modulation of excitability or a resonant extra current. The turbulence is terminated with much higher probability using a resonant frequency perturbation than a non-resonant one. Suppression of the turbulence using a resonant frequency is up to fifty times faster than using a non-resonant frequency, in both the modulation of excitability and the extra current modes. We also demonstrate that resonant perturbation requires strength one order of magnitude lower than that of a single pulse, which is currently used in clinical practice to terminate cardiac fibrillation. Our results provide a robust method of controlling complex chaotic spatio-temporal processes. Resonant drift of spiral waves has been studied extensively in two dimensions, however, these results show for the first time that it also works in three dimensions, despite the complex nature of the scroll wave turbulence.

PACS numbers:

## I. INTRODUCTION

Turbulence of scroll waves is a sort of spatiotemporal chaos that is observed in some three-dimensional (3D) excitable media [1, 2, 3, 4, 5, 6, 7, 8, 9]. In cardiac tissue, such chaotic behaviour is known as fibrillation [10] and implies cardiac failure.

The current method for terminating fibrillation in cardiac tissue is by means of a single electric pulse with a large amplitude. However, this approach is far from ideal. There are several known side-effects linked to the administration of the large electric shocks to patients [11]. Termination of fibrillation using shocks with a lower amplitude would overcome such problems.

Resonant drift of a spiral wave in two dimensions (2D) has been observed when one of the parameters of a model of an excitable medium was changed in time, with the period equal to that of the spiral wave [12, 13]. This phenomenon was later shown to be generic for reaction-diffusion excitable systems [14, 15]. Thus it appeared that resonant drift could be used for moving the spiral wave around the medium to a boundary where it would terminate.

Numerical experiments with reaction-diffusion models revealed that when close to boundaries, the period of the spiral wave changes, thus destroying the resonance in such a way that the drift trajectory turns away from the boundary. The main reason for this unruly behaviour is “resonant repulsion”, caused by the untuning of the resonance between the spiral and the perturbation, due to the variation of the spiral’s own frequency [14, 15]. This can be rectified by adjusting the frequency of the external forcing accordingly, based on some kind of feedback

obtained from the re-entry itself. Feedback control of the resonant drift has been shown to overcome repulsion from the boundaries and inhomogeneities [15, 16]. The same method can also eliminate multiple spiral waves, thus demonstrating that multiplicity of re-entrant sources in fibrillation is not in itself an obstacle for low-voltage defibrillation by this method [15].

Chambers of a heart, particularly ventricles, are 3D, so termination of scroll waves should be studied. Scroll wave turbulence presents a new challenge for resonant drift control, since here we are dealing not only with multiple sources, but sources that tend to multiply.

A scroll wave rotates around a central filament. Depending on the parameters of the medium, a filament of a circular shape may gradually contract or expand with time [1, 17]. For filaments of arbitrary shape, this property translates into “filament tension” [2].

In excitable media, if a circular filament contracts, then a filament of any shape in the same medium has “positive tension” and will shorten with time. Scroll waves with positive filament tension therefore either collapse or stabilise to a straight shape. In a bounded medium this can lead to the self-termination of the scroll.

If a circular filament expands, then any filament shape is unstable as the filament has “negative tension” and will tend to lengthen. It was therefore conjectured [1, 2, 3] and subsequently demonstrated [4, 7, 8, 9] that such excitable media of sufficiently big size should support “turbulence” of scroll waves, where the scroll filaments grow, spontaneously bend, and break up to fragments upon collision with boundaries and with each other. Negative filament tension is not the only mechanism of scroll wave turbulence: similar behaviour may occur due to

non-uniform anisotropy of diffusivity, like that found in a ventricular wall [5, 6].

Alonso *et al.* [7] considered the effect of applying a periodic *non-resonant* forcing on scroll wave turbulence produced by negative filament tension. By numerical simulations of the Barkley model, they showed that periodic modulation of the medium’s excitability with constant frequency higher than the frequency of the scroll waves can control the turbulence in the medium. They went on to propose a theory of this effect, based on the “kinematic description” of the scroll waves [18]. Their interpretation is that faster-than-resonant stimulation can effectively change the filament tension from negative to positive, thus disrupting the mechanism supporting the multiplication of scroll filaments, and compelling them to collapse.

However, to our knowledge, the possibility of eliminating scroll turbulence by *resonant* stimulation has not been investigated so far. We set this task for the present study.

In this study we compare suppression of the scroll wave turbulence using (1) modulation of the medium’s excitability, as used by Alonso *et al.* in [7], to enable comparison of our resonant forcing results with their non-resonant forcing, and (2) an “extra transmembrane current” forcing, as in [15]. Keeping in mind single shock cardiac defibrillation used in clinical practice, we also compare repetitive external forcing of constant and feedback controlled frequencies to a single pulse extra current forcing.

Our results show that resonant perturbation ensures the quickest termination of the scroll wave turbulence. Feedback controlled external perturbation was as effective as constant frequency resonant perturbation, but offers the advantage of not having to know the correct frequency *a priori*. The resonant and feedback-controlled forcing suppress the 3D turbulence using amplitudes one order of magnitude lower than that of a single pulse currently used in clinical practice to terminate fibrillation.

## II. METHODOLOGY

### A. Governing Equations

The 3D numerical simulations presented here were performed using the Barkley model of excitable media [19],

$$\frac{\partial u}{\partial t} = \frac{1}{\epsilon} u(1-u) \left( u - \frac{v+b(t)}{a} \right) + \nabla^2 u + h(t), \quad (1)$$

$$\frac{\partial v}{\partial t} = u - v, \quad (2)$$

where  $\epsilon$  is a small parameter  $\epsilon \ll 1$  characterising mutual time scales of the fast  $u$  and slow  $v$  variables, and  $a$  and  $b$  specify the kinetic properties of the system. Parameter  $b$  determines the excitation threshold and thus controls the excitability of the medium. The term  $h(t)$  represents an “extra transmembrane current”.

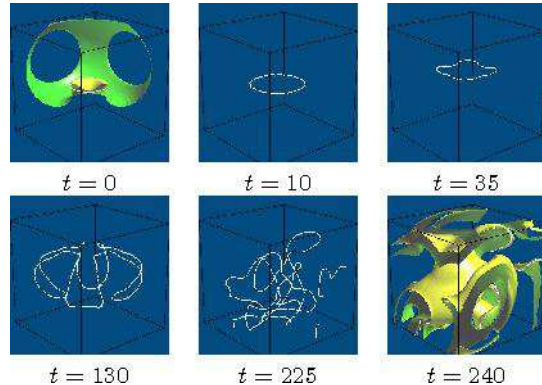


FIG. 1: (color online) Development of scroll wave turbulence from an initial scroll ring. The white lines show the filaments of the scroll waves.

### B. Numerical Methods

For numerical simulations, we used EZscroll software by Barkley *et al.* [19, 20], modified appropriately to describe the stimulation. We used a 19-points finite difference approximation of the Laplacian with equal discretization steps  $\Delta x$  in all three spatial directions, and an implicit first order Euler time stepping with a time step  $\Delta t$ . Simulations were run in a box  $(x, y, z) \in [0, L]^3$ , with Neumann boundary conditions. In most simulations, we used  $\Delta x = 2/3$ ,  $\Delta t = 1/30$  and  $L = 60$ .

In all simulations the model parameters were chosen as  $a = 1.1$ ,  $b = 0.19$  (or the average value of  $b(t)$  when it varied), and  $\epsilon = 0.02$ , as in [7]. At this set of parameters a scroll wave will have negative filament tension.

The choice of parameters was the same as in [7] to allow comparison, with the exception of the discretization steps. We used cruder discretization steps, which allowed us to perform more simulations within reasonable CPU time. We performed also selected control simulations with  $\Delta x = 0.4$ ,  $\Delta t = 0.01$  and  $L = 60$ , as in [7]; the results were quantitatively somewhat different but qualitatively similar (see below for details).

### C. Generation of turbulence

The development of scroll wave turbulence is presented in fig. 1. Starting at  $t = 0$  with the standard EZScroll scroll ring initial conditions in an unperturbed medium, the negative tension of the initial scroll ring caused elongation and bending of the filament. Interaction with the boundaries caused the filament to fragment and soon a complex tangle of many filaments filling the volume was observed.

The turbulent state of the system was saved at five different times  $t = 240, 245, 250, 255, 260$ , and then each state used as an initial condition in our simulations.

## D. Resonant Frequency

There are different ways to define resonance between the forcing and the turbulence it is aimed to control. We considered three different frequencies, to which the forcing frequency can be compared:

- The rotation frequency of an unforced vortex around its filament  $\omega_0$ . It is also the frequency of a 2D spiral wave in a large enough medium. It is typically used as the leading-order approximation in any perturbative theoretical approaches, as [2, 7].
- The mean frequency of the unforced turbulence  $\bar{\omega}_0$ . It is different from  $\omega_0$  due to interaction of scrolls with each other and with boundaries. This difference can be significant as this interaction is the only factor that stops the filaments' growth in length and number.
- The mean frequency of the forced turbulence  $\tilde{\omega}_0(A, \omega_f)$ , which depends on the forcing amplitude  $A$ , and the forcing frequency  $\omega_f$  (see fig. 2(a,b)). By definition,  $\tilde{\omega}_0(0, \omega_f) = \bar{\omega}_0$  for any  $\omega_f$ . The difference between  $\tilde{\omega}_0$  and  $\bar{\omega}_0$  is less obvious from the theoretical viewpoint than the difference between  $\bar{\omega}_0$  and  $\omega_0$ , as the theory of resonant drift of the scroll wave turbulence is yet to be developed. Yet we suppose that it is  $\tilde{\omega}_0$  that is to be compared to the forcing frequency to determine resonance, since it represents the *de facto* state of the controlled system regardless of the detailed mechanisms that brought it into that state.

The frequency  $\omega_0$  was measured for a single straight scroll. The frequencies  $\bar{\omega}_0$  and  $\tilde{\omega}_0(A, \omega_f)$  were both measured by recording the intervals  $T_j$  between the moments  $t_j^r$  in which wavefronts passed through a recording point  $(x_r, y_r, z_r)$ , that is,  $T_j = t_{j+1}^r - t_j^r$ ,  $u(x_r, y_r, z_r, t_j^r) = u_*$ , where  $u_* = 0$ , and  $\frac{\partial u}{\partial t}(x_r, y_r, z_r, t_j^r) > 0$ . The mean frequency for the entire simulation was then calculated as the average,  $\bar{\omega}_0 = 2\pi/\langle T_j \rangle = 2\pi N / \sum_{j=1}^N T_j$ , for all  $N$  intervals recorded, and similarly for  $\tilde{\omega}_0$ . For  $\bar{\omega}_0$  the simulation was run for  $t \in [0, 5000]$ . For  $\tilde{\omega}_0(A, \omega_f)$  the simulation was run for  $t \in [0, 5000]$  or until all scrolls were terminated if it happened sooner.

For our crude discretization steps  $\Delta x = 2/3$ ,  $\Delta t = 1/30$  and  $L = 40$ , when modulating the medium's excitability we have observed  $\omega_0 = 0.90$ ,  $\bar{\omega}_0 = 1.05$  and  $\tilde{\omega}_0(0.03, \omega_0) = 0.74$ . The finer discretization steps  $\Delta x = 0.40$ ,  $\Delta t = 0.01$  and  $L = 60$  produced  $\omega_0 = 1.20$ ,  $\bar{\omega}_0 = 1.27$  and  $\tilde{\omega}_0(0.03, \omega_0) = 1.01$ . That is, the cruder discretization slows down the scroll waves overall, compared to the finer discretization, but the relationship between the key frequencies remains similar.

## E. Forcing

We investigated the application of the following types of forcing on scroll wave turbulence;

1. Modulation of the medium's excitability, *i.e.* variation of parameter  $b(t)$  around its average value  $b_0$ .
  - (a) Repetitive stimulation
    - i. Constant frequency
2. Extra transmembrane current,  $h(t)$ 
  - (a) Single pulse
  - (b) Repetitive stimulation
    - i. Constant frequency
    - ii. Feedback controlled

### 1. Modulation of the medium's excitability

The medium's excitability in the model is defined by parameter  $b$ . Following [7, 18], we introduced into the model a spatially-uniform forcing by applying a periodic modulation of the parameter  $b$  in time, while keeping the extra current term zero,

$$b(t) = b_0 + A \cos(\omega_f t), \quad h(t) = 0, \quad (3)$$

where  $b_0 = 0.19$ ,  $A$  is the forcing amplitude, and  $\omega_f$  is the forcing frequency. Since  $b$  determines the excitation threshold, varying its value will vary the excitability of the medium.

Starting from the five different turbulent initial conditions, the simulations were performed at different values of  $A$  and  $\omega_f$ , and the time taken for elimination of the turbulence was recorded. If any scrolls remained after  $t = 5000$  then the experiment was stopped and considered to have failed to eliminate the turbulence.

### 2. Extra transmembrane current

Here, simulations were performed with

$$b(t) = b_0 = 0.19, \quad h(t) \neq 0.$$

(a) *Single pulse.* Simulations were started from the saved initial conditions at  $t = t_0$  and a single pulse of time duration  $\Delta = 0.3$  was applied,

$$h(t) = A \Theta(t - t_0) \Theta(t_0 + \Delta - t),$$

where  $\Theta()$  is the Heaviside step function. After the shock, evolution of the filaments was observed for a further 250 units of time. If no filaments remained at the end of this period, the shock was considered to be a success, and otherwise it was deemed to be unsuccessful.

Shocks of different amplitudes  $A$  were tested, and the success threshold was defined as the amplitude which gives a 50% success rate over the five initial conditions used.

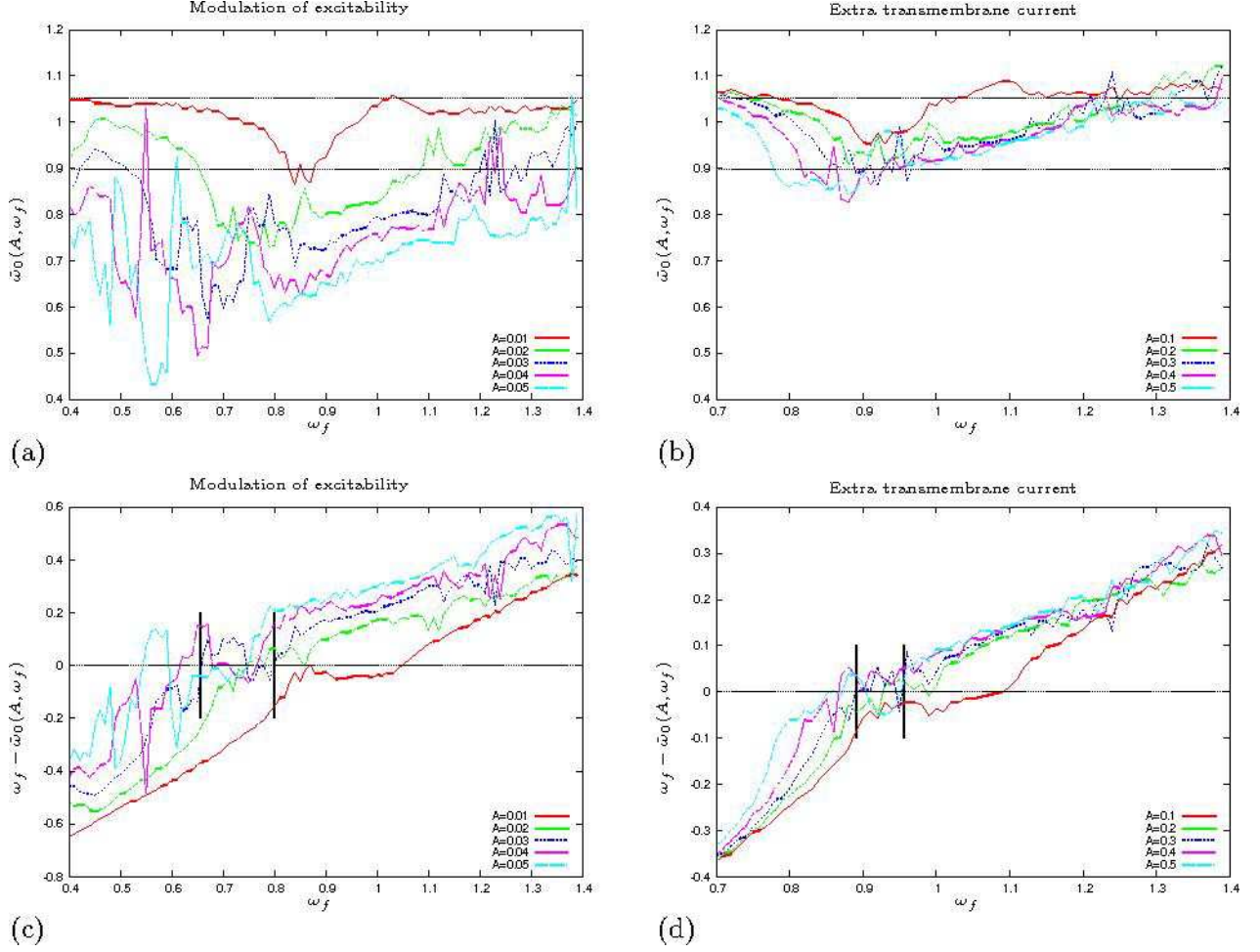


FIG. 2: (color online) The mean frequency  $\tilde{\omega}_0(A, \omega_f)$  of the perturbed turbulence, measured at the point  $(x_r, y_r, z_r) = (0, 0, 0)$ , against forcing frequency  $\omega_f$  at different forcing amplitudes  $A$  due to (a) modulation of the medium's excitability and (b) extra transmembrane current forcing. In (a) and (b) the line  $\bar{\omega}_0 = 1.05$  is the mean frequency of the unperturbed turbulence, and the line  $\omega_0 = 0.9$  is the frequency of the single vortex. The **resonant windows** can be seen from the deviation of the mean frequency  $\tilde{\omega}_0(A, \omega_f)$  from the forcing frequency  $\omega_f$  due to (c) modulation of excitability and (d) extra current forcing. In (c) and (d) the line  $\omega_f - \tilde{\omega}_0(A, \omega_f) = 0$  is drawn to highlight the resonant windows. The vertical brackets illustrate the corresponding resonant windows at forcing amplitude  $A = 0.03$  for (c) and  $A = 0.3$  for (d).

(b) *Repetitive stimulation.* The stimulus  $h(t)$  was set to be a repetitive series of rectangular pulses of amplitude  $A$ ,

$$h(t) = A \sum_{j=1}^N \Theta(t - t_j^s) \Theta(t_j^s + \Delta - t).$$

We studied the effect of repetitive stimulation with both constant and feedback-controlled frequencies.

### i. Constant frequency

Simulations were started from the saved initial conditions at  $t = t_0$ , and periodic pulses were applied,  $t_j^s = t_0 + j 2\pi/\omega_f$ ,  $j = 0, 1, 2, \dots$ . Experiments were repeated for different forcing frequencies  $\omega_f$  and amplitudes  $A$ , and the time taken to eliminate the turbulence in each experiment was recorded. If

any scrolls remained after  $t = 5000$  then the experiment was stopped and considered to have failed to eliminate the turbulence.

### ii. Feedback controlled

Stimulation  $h(t)$  was set to be a repetitive series of rectangular pulses with timings  $t_j^s$  determined by taking feedback from the turbulence itself. Feedback is taken from a recording point  $(x_r, y_r, z_r)$  so that a pulse is applied every time that a wave passes through this point, that is,  $t_j^s = t_j^r + t_{\text{delay}}$ ,  $u(x_r, y_r, z_r, t_j^r) = u_*$  and  $\frac{\partial u}{\partial t}(x_r, y_r, z_r, t_j^r) > 0$ . We also varied the time delay  $t_{\text{delay}}$  for applying a pulse after a wavefront has passed through the recording point. Delays ranging from  $t_{\text{delay}} = 0.0$  to  $t_{\text{delay}} = 6.0$  were used, with increments of 0.1.

Different locations were used for the recording point



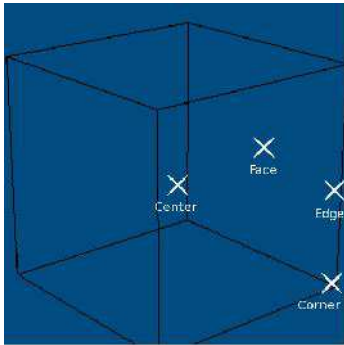


FIG. 3: (color online) Different locations for the recording point

(see fig. 3):

- in the **corner** of the domain,  $(x_r, y_r, z_r) = (0, 0, 0)$ ,
- in the **center** of the domain,  $(x_r, y_r, z_r) = (L/2, L/2, L/2)$ ,
- in the center of a **face** of the domain,  $(x_r, y_r, z_r) = (L/2, L/2, 0)$ ,
- in the center of an **edge** of the domain,  $(x_r, y_r, z_r) = (L/2, 0, 0)$ .

Experiments were repeated for different locations for the recording point, different values of time delay  $t_{\text{delay}}$ , and amplitude  $A$  and the time taken for the elimination of the turbulence recorded. If any scrolls remained after  $t = 5000$  time steps, then the experiment was stopped and considered to have failed to eliminate the turbulence.

### III. RESULTS

#### A. Elimination of the turbulence

Fig. 4 illustrates the main result of our study: a resonant stimulation can eliminate scroll wave turbulence, and does it quicker and more reliably than a non-resonant stimulation. The figure shows evolution of the turbulence due to modulation of the medium’s excitability at three different forcing frequencies at a fixed amplitude. The forcing frequency  $\omega_f = 0.8$  is within the “resonant window” (see below for a formal definition), and the turbulence is terminated quickly within  $t = 41$ . The forcing frequency  $\omega_f = 1.22$  is above-resonant, and although the turbulence is terminated, it takes much longer,  $t = 2089$ . The forcing frequency  $\omega_f = 1.13$  is also above the resonant window, and it leads to stabilisation of vortices in the center of the medium rather than their termination.

We note here that the mechanism of “taming” of scroll wave turbulence suggested by Alonso *et al.* [7, 18] is based on inversion of the filament tension from negative to positive. The sequence shown in fig. 4(c) illustrates why this

is *not* sufficient for defibrillation: the scroll filaments stabilise with a straight shape, which is consistent with their effective tension being positive, but it does *not* lead to their elimination.

In the following subsections, we analyse in more details the empirical conditions required for successful termination of the turbulence.

#### B. Windows of resonant frequencies

For both the modulation of the medium’s excitability and extra transmembrane current forcing, we have varied the frequency  $\omega_f$  and amplitude  $A$  to assess their effects on termination of the turbulence. We observed very different effects of the modulation of excitability and of the extra current forcing on the mean frequency of the turbulence  $\tilde{\omega}_0(A, \omega_f)$ . In this section we define a resonant window of frequencies for each amplitude and forcing type.

##### 1. Modulation of excitability

As the amplitude of the modulation increases, the mean frequency of the turbulence  $\tilde{\omega}_0(A, \omega_f)$  decreases dramatically (see fig. 2(a)). When using the largest forcing amplitude ( $A = 0.05$ ), the frequency of the turbulence reduced to over half that of the frequency of the unperturbed turbulence.

Resonant windows can be identified in fig. 2(c). We define the resonant window to be the range of forcing frequencies  $\omega_f$ , for which  $\omega_f \approx \tilde{\omega}_0(A, \omega_f)$ . The upper and lower bounds for the resonant window can be seen as the first and last points where  $\omega_f - \tilde{\omega}_0(A, \omega_f) = 0$ . The resonant window is taken to be this range and a further 0.01 either side of this range.

There is a different resonant window for each amplitude. As the amplitude increases, the size of the resonant window increases and shifts towards lower forcing frequencies.

The above definition of the resonant window should be used with caution for the lowest amplitudes. E.g. for  $A = 0.01$  in Fig.2(c) the window must be between 0.873 and 1.045. However, most of this interval corresponds to a “false resonance”, when  $\omega_f \approx \tilde{\omega}_0$  but that does not lead to termination. Termination of the turbulence at this forcing amplitude is observed in the narrow vicinity of  $\omega_f = 0.873$  only. Applying a forcing with frequency in the vicinity of  $\omega_f = 1.045$  maintains the turbulence.

##### 2. Extra transmembrane current

As the amplitude of the extra current forcing increases, the mean frequency of the turbulence  $\tilde{\omega}_0(A, \omega_f)$  decreases (see Fig.2(b)), though not so dramatically as in the case of modulation of the medium’s excitability, compare Fig.2(a) and (b). Even for the largest forcing amplitude

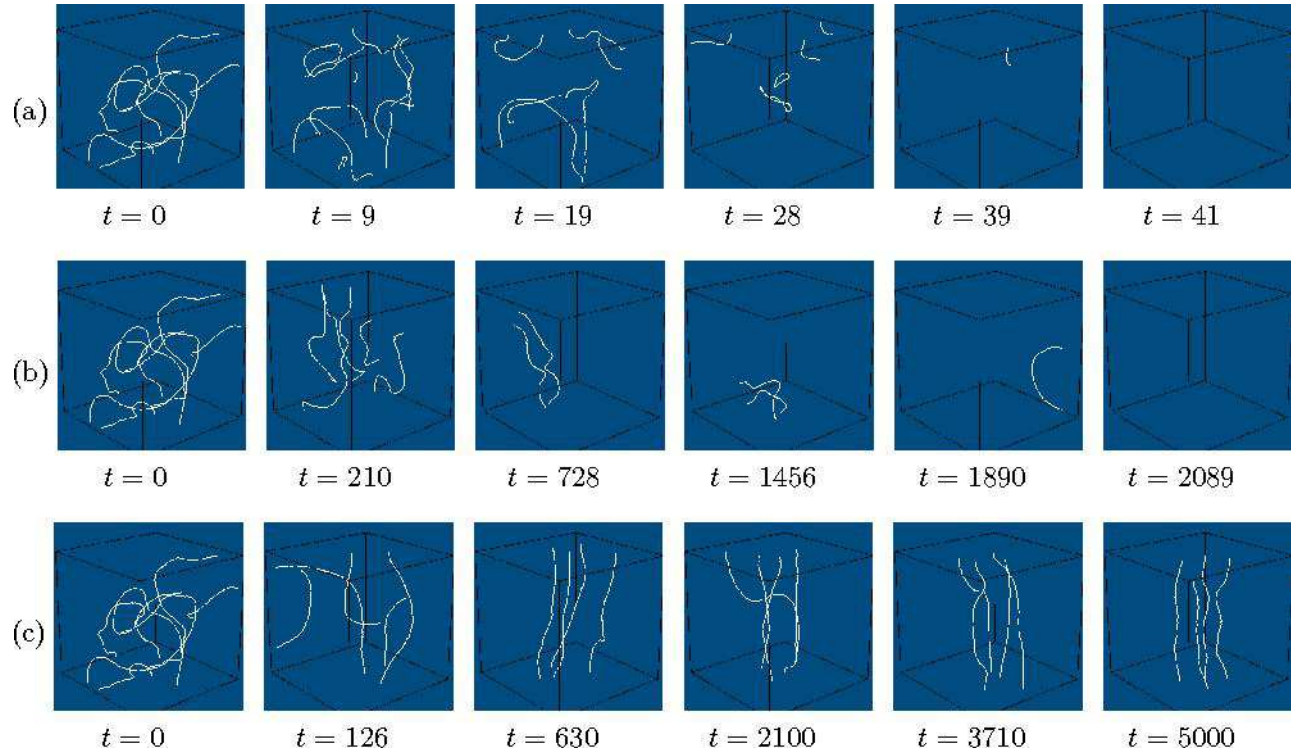


FIG. 4: (color online) Examples of successful and unsuccessful elimination of turbulence. Evolution of the turbulence under modulation of medium excitability with (a)  $\omega_f = 0.8$ , (b)  $\omega_f = 1.22$ , (c)  $\omega_f = 1.13$  at fixed amplitude  $A = 0.03$ .

$A = 0.5$ , the reduction in the frequency of the turbulence due to the extra current forcing is not more than 20% of the frequency of the unperturbed turbulence.

Resonant windows for extra current forcing can be identified in Fig.2(d). The resonant windows were defined in the same way as in section III B 1. There is a different resonant window for each amplitude, although for all forcing amplitudes that we tested, the resonant windows are in the vicinity of the frequency of a straight scroll  $\omega_0 = 0.9$ .

For the lowest amplitude  $A = 0.1$  in Fig.2(d) there is no obvious resonant window. However, the resonant termination of the turbulence at this forcing amplitude is observed in the narrow vicinity of 0.870. The interval of frequencies above that and up until 1.09 corresponds to the “false resonance”.

### C. Termination times

#### 1. Modulation of the medium’s excitability

Fig. 5 presents the turbulence termination times due to modulation of the medium’s excitability at four different forcing amplitudes. The vertical brackets show the windows of resonant frequencies for each amplitude, as in fig. 2. From these data, it can be seen that termination of turbulence is fastest when the forcing frequency  $\omega_f$  is within the resonant window. The turbulence can be

terminated with a frequency outside of the resonant window. Although, further away from the resonant window, average termination time increases and the probability of success decreases.

Fig. 6 shows a plot of termination time against (a) fixed forcing amplitude  $A$ , and (b) untuning of the resonance  $\delta$  defined as:

$$\delta = \frac{|\omega_f - \tilde{\omega}_0(A, \omega_f)|}{\sigma},$$

where  $\sigma$  is the standard deviation of the turbulence frequency recorded throughout a simulation,

$$\sigma = 2\pi \left( \frac{1}{N} \sum_{j=1}^N T_j^{-2} - \left( \frac{1}{N} \sum_{j=1}^N T_j^{-1} \right)^2 \right)^{1/2}.$$

The strength of resonance is a measure of how close the forcing frequency is to the frequency of the scroll wave turbulence.

It can be seen from fig. 6(a) that increasing  $A$  reduces the termination time. The reduction is not very pronounced at larger  $A$ ; one should bear in mind here that the data in this graph are for *all* frequencies, resonant or not. Fig. 6(b) shows that at smaller  $\delta$ , *i.e.* a better resonance, the time taken to eliminate the turbulence reduces. Here the data are for all forcing amplitudes, large and small. Comparing fig. 6(a) and fig. 6(b), and taking into account that reliable forcing amplitudes for the the

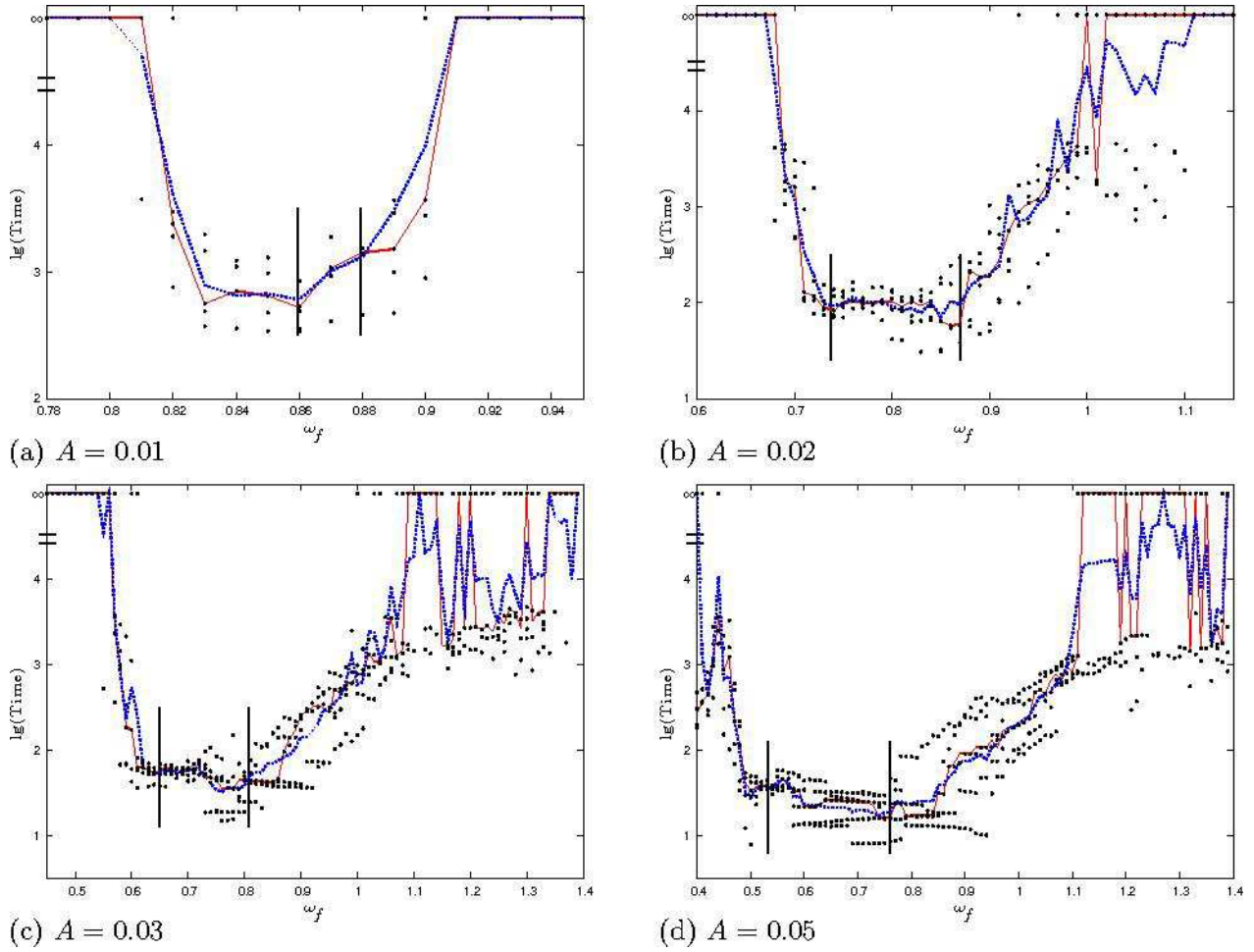


FIG. 5: (color online) Modulation of medium's excitability: termination times at different amplitudes: (a)  $A = 0.01$ , (b)  $A = 0.02$ , (c)  $A = 0.03$  and (d)  $A = 0.05$ . Black dots: termination times for individual simulations. Red solid line: median values of the termination times at every fixed frequency. Blue dashed line: same, geometric mean values. For averaging and visualization purposes, we assign value  $t = 10^5$  to the failures. Black vertical brackets: the windows of resonant frequencies for each amplitude.

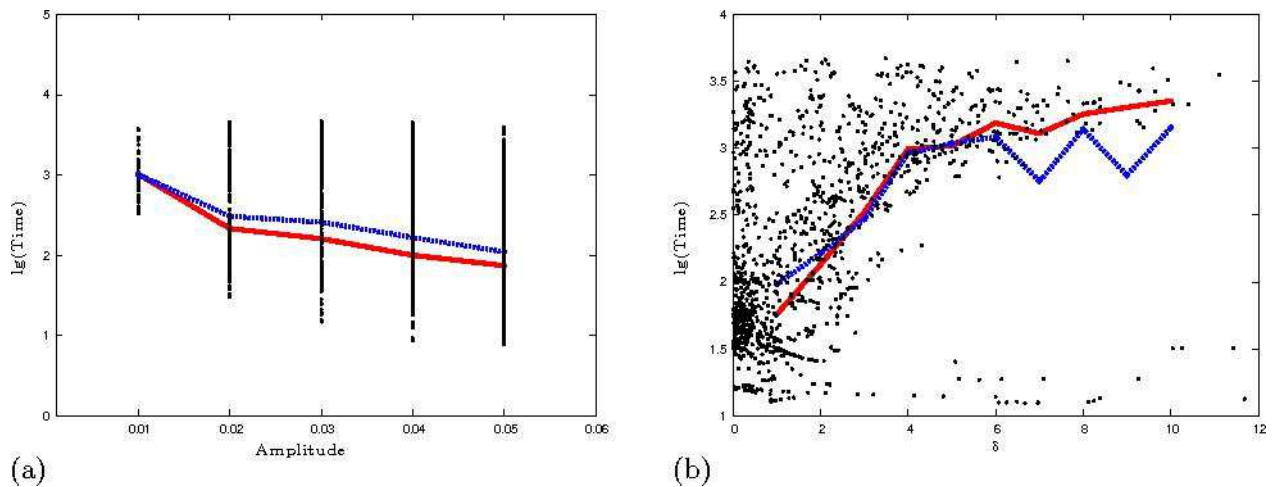


FIG. 6: (color online) Modulation of medium's excitability: Termination time against (a) fixed forcing amplitude  $A$ , (b) untuning of the resonance  $\delta$ . The dots represent termination times for individual simulations. The solid line goes through the median values of the termination times at either (a) or (b), and the dashed line through the geometric mean values.

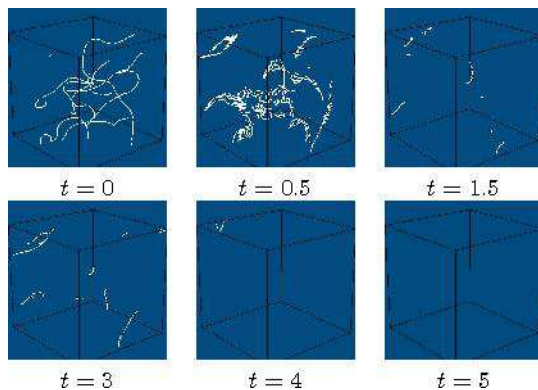


FIG. 7: (color online) Single pulse: termination of the turbulence at forcing amplitude  $A = 4.3$ .

turbulence termination seems to be  $A \geq 0.02$ , termination times are more sensitive to the quality of resonance than to the forcing amplitude.

## 2. Extra transmembrane current forcing

(a) *Single pulse.* The single pulse stimulation was tested having in mind the current clinical practice for cardiac defibrillation is by means of a single electric pulse of large amplitude. We defined the single pulse success threshold as the amplitude at which the turbulence is terminated in more than 50% of the experiments. In our setup, this success threshold was found to be  $A = 4.3$ . Fig. 7 shows an example of successful defibrillation with a single pulse shock at amplitude  $A = 4.3$ .

(b) *Repetitive pulses.* Fig. 8 presents the turbulence termination times, both for constant-frequency and feedback-controlled extra current forcing. The solid-line and dashed-line curves show the dependence of the termination times on the extra current forcing frequency  $\omega_f$ , at fixed amplitude  $A = 0.3$ . The vertical brackets show the window of resonant frequencies as in fig. 2(d). The dashed horizontal straight line shows the geometric mean termination time for the feedback controlled stimulation, and the solid horizontal line shows the corresponding median termination time. From these data, it can be seen that forcing frequencies within the resonant window ensure the fastest termination of turbulence. The turbulence can be terminated with a frequency outside of the resonant window but there the probability of the turbulence termination decreases. The individual experiments with failed termination are depicted as  $\log_{10}(t) = \infty$ , and counted for the sake of averaging as  $\log_{10}(t) = 5$ . Further away from resonant frequencies the turbulence termination time rapidly increases.

Fig. 9 illustrates the effects of the stimulation amplitude  $A$ . The left panels in it are similar to fig. 8 and present the turbulence termination time dependence on the extra current forcing frequency  $\omega_f$ , at four different amplitudes  $A = 0.1, 0.2, 0.4, 0.5$ . The histograms on

the right show the distributions of termination times for feedback controlled experiments, for the four different locations of the recording point. All the observations made for fig. 8 are valid for the forcing amplitudes in fig. 9.

For amplitudes  $A > 0.2$  in feedback controlled experiments, the average termination time is close to the average termination time achieved at resonant frequencies. For lower amplitudes, the success probability using feedback-controlled stimulation falls down, in the same way as it does for the constant-frequency forcing.

The location of the recording point used for the feedback is also important for a successful termination. The most successful locations, in the 3D experiments, appear to be the corner or the edge of the medium. The center location for the recording point appears to be the worst for all forcing amplitudes tested.

Fig. 10 shows evolution of the turbulence due to extra current forcing at different forcing frequencies  $\omega_f = 0.9, 1.22, 1.15$ , and the feedback controlled, at the fixed amplitude  $A = 0.3$ . The forcing frequency  $\omega_f = 0.9$  is within the resonant window, and the turbulence is terminated quickly by  $t = 134$  (series a). The feedback controlled stimulation terminates the turbulence by  $t = 190$  (series b). The forcing frequency  $\omega_f = 1.22$  is above-resonant, although the turbulence is terminated it takes ten times longer, to  $t = 1773$  (series c). The forcing frequency  $\omega_f = 1.15$  is also above the resonant window. Simulation with that frequency leads to stabilisation of a vortex in the center of the medium (series d), similar to what was observed for faster-than-resonant modulation of excitability, see fig. 4(c).

Fig. 11 is similar to fig. 6 and shows plots of termination time against (a) fixed forcing amplitude  $A$ , and (b) untuning of the resonance  $\delta$ , defined in the same way as for the modulation of excitability forcing. It can be seen from fig. 11(a) that increasing the amplitude  $A$  reduces the termination time. Fig. 11(b) shows that reducing the untuning  $\delta$  also reduces the termination time. Comparing fig. 11(a) and fig. 11(b), and taking into account that reliable forcing amplitudes for the turbulence termination seems to be  $A \geq 0.2$ , termination times are more sensitive to the untuning of resonance  $\delta$  than to the change of forcing amplitude  $A$ .

## IV. DISCUSSION

### A. Resonant stimulation terminates scroll turbulence

We have shown that a termination of the scroll wave turbulence can be achieved by repetitive stimulation. This is despite the fact that scroll waves continue to grow and multiply while we drive them to elimination. We have studied two different methods of forcing, the modulation of medium's excitability and the extra transmembrane currents forcing. Where comparable, the qualita-



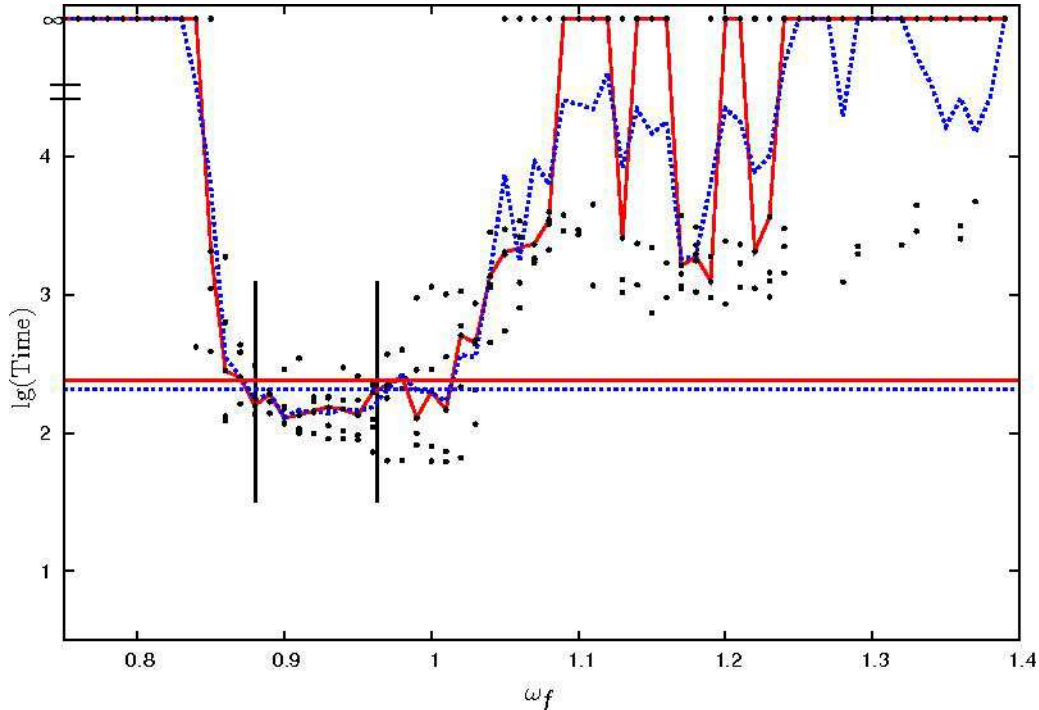


FIG. 8: (color online) Extra current forcing: termination time for the amplitude  $A = 0.3$ . The black dots represent termination times for individual simulations. The red solid line goes through the median values of the termination times at a fixed frequency, and the blue dashed line through the geometric mean values. The horizontal straight lines show the median (red solid line) and geometric mean (blue dashed line) termination times for the feedback experiments. The vertical brackets designate the window of resonant frequency.

tive dependencies for the two methods were similar. For a successful termination, the amplitude of the repetitive forcing should be higher than a certain threshold. However, this threshold is still much lower than that required for termination by a single shock. The termination is achieved with the highest probability, and in the quickest time, when using a resonant forcing frequency, *i.e.* when the frequency of stimulation,  $\omega_f$ , is close to the *de facto* frequency of the forced scroll waves,  $\tilde{\omega}_0(A, \omega_f)$ . Namely, we have shown that for both types of forcing, the turbulence termination becomes faster for smaller values of the untuning of the resonance  $\delta$  (see fig. 6(b) and fig. 11(b)).

### B. Resonant windows

We have found that the resonance between the forcing and the scrolls is characterised not by a single resonant frequency, but by a resonant window which depends on the type of forcing and its amplitude. For the modulation of the medium's excitability, larger amplitudes corresponded to wider resonant windows, shifted towards lower forcing frequencies. For the extra transmembrane current forcing, the resonant windows did vary in size and location, but for the amplitudes that we tested they remained close to the frequency of a single straight vortex,  $\omega_0 \approx 0.9$ .

Our results also show that for both modulation of excitability and extra current forcing, the fastest termination was achieved when the forcing was applied with a frequency chosen within the resonant window. Termination using a forcing frequency outside of the resonant window occurs with a much lower probability and a longer termination time.

Existence of resonant windows rather than unique resonant frequencies may be a purely statistical phenomenon due to fluctuations of frequencies of the scroll turbulence, or may be an indication that the forced turbulence adjusts its frequency in response to the forcing, *i.e.* a “frequency locking” in average (perfect locking is not feasible between a periodic forcing and chaotic turbulence). Nothing like this has been reported for resonant drift in 2D, thus we may be dealing with a specifically three-dimensional phenomenon. Indeed, 3D scrolls have additional degrees of freedom compared to 2D spirals, *e.g.* twisted scrolls can rotate faster than straight scrolls [21, 22]. This might offer an explanation of cases of false resonance, when formally defined resonant windows are abnormally extended towards higher frequencies but are not associated with fast and reliable termination, see *e.g.* the case of  $A = 0.01$  in fig. 2(a,c) and fig. 5(a). Indeed, in case of strong twist, different parts of the same filament have different phases and are forced in different directions, which does not result in an overall directed

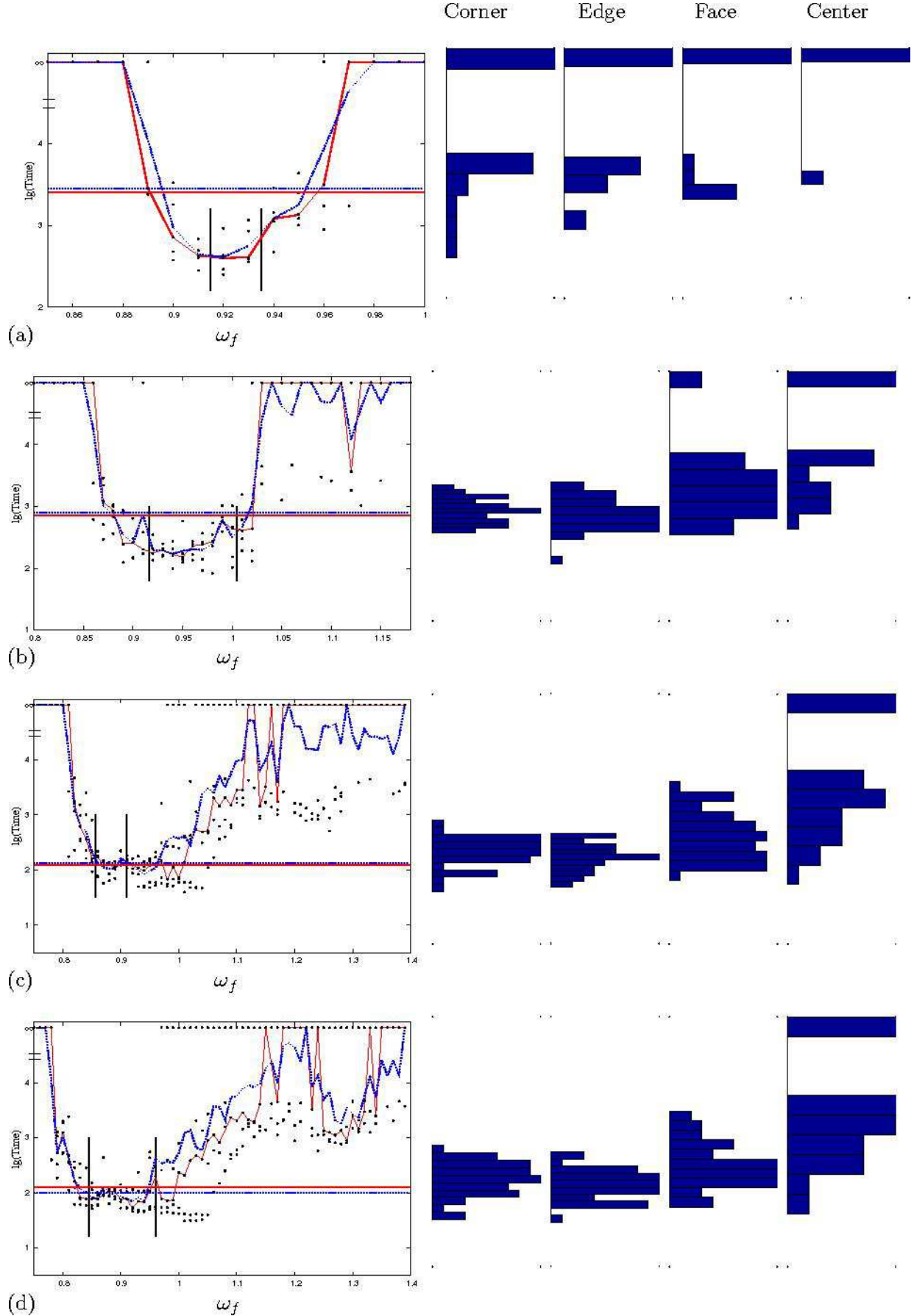


FIG. 9: (color online) Extra current forcing: termination times for the amplitudes (a)  $A = 0.1$ , (b)  $A = 0.2$ , (c)  $A = 0.4$ , (d)  $A = 0.5$ . The left panels are as in Fig.8. The histograms on the right are distribution of termination times for feedback controlled experiments, at different locations for the recording point (they are rotated 90° clockwise and flipped in the vertical

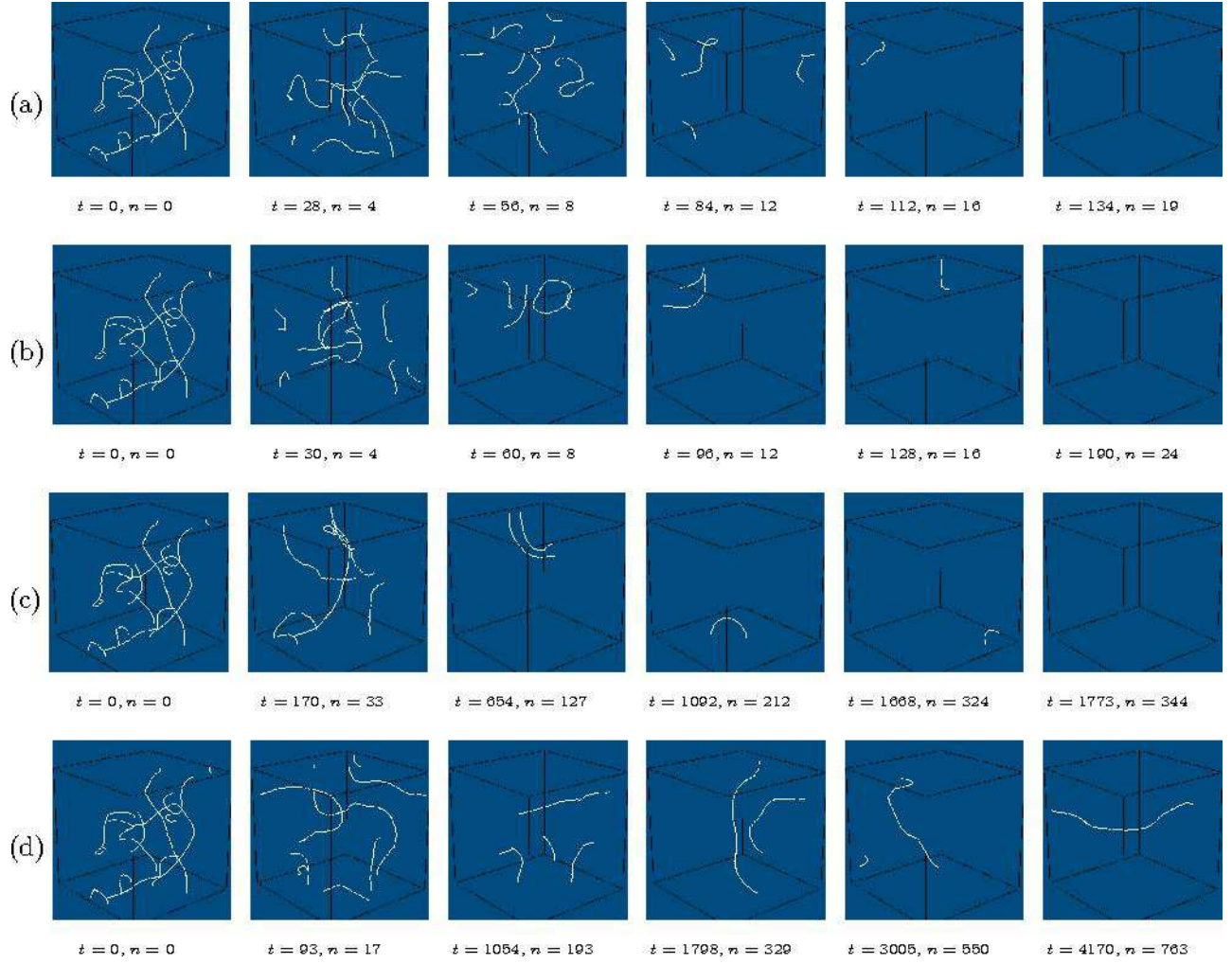


FIG. 10: (color online) Extra current forcing: evolution of the turbulence using (a)  $\omega_f = 0.9$  (b) feedback (c)  $\omega_f = 1.22$  (d)  $\omega_f = 1.15$  at fixed amplitude  $A = 0.3$ .

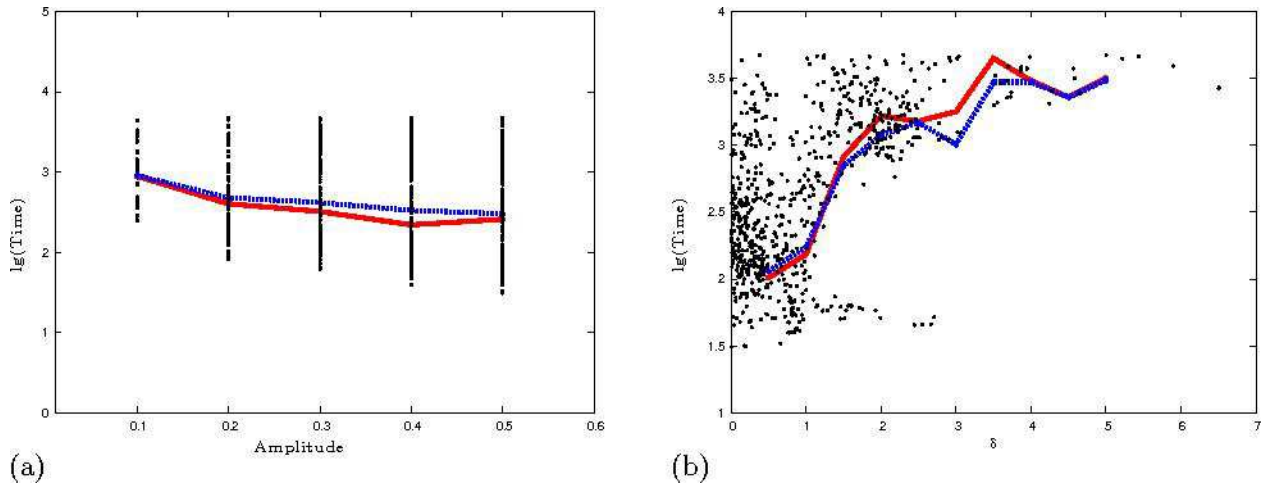


FIG. 11: (color online) Extra current forcing: Termination time against (a) fixed forcing amplitude  $A$ , (b) untuning of the resonance  $\delta$ . The dots represent termination times for individual simulations. The solid line goes through the median values of the termination times at either (a) or (b), and the dashed line through the geometric mean values.

movement and does not bring about termination.

### C. Resonant vs non-resonant stimulation

It has been previously shown [7] in Barkley’s model with the same model parameters as we used here, that scroll wave turbulence can be controlled by a weak *non-resonant* modulation of the medium’s excitability. A theory was presented in [18] explaining that this control of turbulence was due to an inversion of the filament tension from negative to positive, which can happen if the frequency of forcing is higher than the frequency of the scrolls. It was argued that such stimulation causes the filaments to collapse and could therefore be used for termination of the scroll wave turbulence. We have seen, however, that positive tension may lead to stabilization rather than termination of scrolls, see fig. 4(c) and 10(d).

In [7] an above-resonant frequency forcing was used to control the turbulence. More specifically, their forcing frequency  $\omega_f$  was almost equal to (1% higher than) the frequency of a straight scroll,  $\omega_0$ . The frequency of a forced turbulence is significantly lower than the frequency of a straight scroll, *e.g.*  $\tilde{\omega}_0(A, \omega_0) < \omega_0$ , thus forcing with frequency  $\omega_0$  is above-resonant. This is true both for the finer discretization steps used in [7] and cruder discretization steps used in a majority of our simulations.

To make a specific comparison, let us consider excitability modulation with amplitude  $A = 0.03$  (same as in [7]) and frequency  $\omega_f = 0.91$  which is about 1% higher than  $\omega_0$ . As can be seen from fig. 5(c), such forcing gives a mean turbulence termination time of  $t = 251$  (compare with termination time  $t = 1510$  in the example shown in [7]). Within the resonant window for this amplitude as defined in this article, the mean termination time is between  $t = 71$  and  $t = 32$ , *i.e.* 3 to 7 times faster than using above-resonant forcing frequency as in [7].

So, a direct like-for-like comparison shows that although the above-resonant frequency stimulation suggested in [7] works in principle, the resonant stimulation works more reliably and much faster.

It has been reported by Wu *et al.* [23] that using a travelling-wave modulation of the mediums excitability can control scroll wave turbulence faster than the modulation used in [7]. Fig.6 in [23] clearly shows that the optimum forcing frequency is below the rotation frequency of an unforced vortex  $\omega_0$ . Alas, Wu *et al.* did not control the *de facto* frequencies of the scroll turbulence so it is not possible to interpret their results unambiguously. However, as we have shown here that the resonant frequencies are below  $\omega_0$ , it is quite possible that the real reason for the advantage achieved in [23] compared to [7] is not (only) in using travelling waves, but simply in using a frequency within a resonant window. A definitive answer to this question requires further investigation.

### D. Feedback control works in 3D

As the resonant window may not be known *a priori*, we tested a simple algorithm for the feedback control with the extra current forcing. It has been previously shown in 2D that applying a repetitive feedback controlled forcing causes a spiral wave to drift to a boundary along a predictable trajectory [15, 16], and possibly terminating it faster than with the constant frequency forcing, as feedback forcing can overcome the “resonant repulsion” of the drifting spirals from boundaries and inhomogeneities [14]. Simulations of spiral waves in the two-dimensional version of our model easily demonstrate resonant repulsion (see fig. 12(a)), so it must play some role in 3D behaviour as well, even though it may be not straightforward in scroll turbulence. Our 3D experiments show that the termination with a feedback-controlled forcing is nevertheless achievable even at relatively weak amplitudes.

Our results also show that the location of the recording point is important for a successful feedback-controlled termination, which is in good agreement with earlier observations of feedback-driven resonant drift in two dimensions [24, 25]. The most successful locations, in the 3D experiments, appear to be the corner or the edge of the medium. The center location for the recording point appears to be the worst for all forcing amplitudes tested. It has been shown in 2D experiments [26] that a line of recording points is a robust approach. Therefore, if the same holds for 3D, a line of recording points down one edge of the medium may be the optimal choice.

### E. Feedback controlled vs constant frequency stimulation

Typically, the average termination time using feedback is close to that achieved at resonant constant frequencies. At the lowest stimulation amplitudes, both feedback-controlled and constant-frequency termination times increase, and the probability of success decreases.

For a range of frequencies within or near the resonant window, the termination was achieved, on average, quicker than with feedback. To elucidate a possible reason for this difference, we have considered a two-dimensional version of the Barkley model, with the same model parameters and applied the same feedback controlled forcing as in our 3D simulations. We have found that applying a forcing with feedback in this case causes the spiral wave to drift along a rather complicated “snaky” trajectory, shown in fig. 12(b). This behaviour is similar to that described recently by Zykov *et al.* [27, 28], and is caused by an instability, related to the delay between a change of the position or phase of the spiral and its detection by the feedback electrode, due to the distance between them and a finite speed of the waves. Indeed, in fig. 12 the spiral core is more than one wavelength away from the recording point. It can be seen from fig. 12(b) at  $t = 525$  that this resonantly drifting



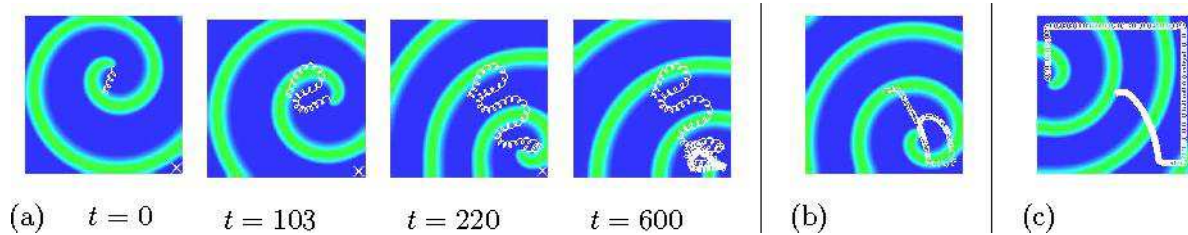


FIG. 12: (color online) Two-dimensional phenomena. (a) ‘Resonant reflection’: Extra current forcing with constant frequency  $\omega_f = 1.1855$  and amplitude  $A = 0.01$ . (b-d) ‘Snake instability’: Extra current forcing with feedback controlled frequency applied with amplitudes  $A = 0.01$  (b),  $A = 0.004$  (c) and  $A = 0.001$  (d). Model parameters  $a = 1.1$ ,  $b = 0.19$ ,  $\epsilon = 0.02$ ,  $L = 60$ ,  $\Delta x = 0.4$  and  $\Delta t = 0.01$ , with 9-point approximation of the Laplacian. The recording point in (b–d) was located in the bottom left corner.

spiral does not terminate at the boundary. Instead, it embarks on a continuous loop near the boundary of the medium.

According to [27, 28], this ‘snake instability’ should disappear at lower amplitudes. Indeed, this is what happened in our simulations, see fig. 12(c,d). The instability was less pronounced when the amplitude is decreased from  $A = 0.01$  in (b) to  $A = 0.004$  in (c), and was completely gone for  $A = 0.001$  in (d). However, although the drift trajectory towards the boundary was shorter, the drift velocity was smaller proportionally to  $A$ , so the time to reaching the boundary did not decrease. Besides, the decrease in  $A$  made annihilation at the boundary even less likely: in (c) the spiral stuck near the boundary similar to (b), whereas at a further reduction of  $A$  in (d) it embarked on a drift along the boundary which was faster than its resonant drift in the center of the domain. So, reducing the amplitude is not necessarily a satisfactory

solution to the problem of the ‘snake instability’ interference with terminating the vortex. Alternative solution could be to reduce the delay in the feedback, say by using a global (ECG) rather than local (point electrogram) signals. However, in known computer models and experimental observations, scroll wave are apparently rather large in the scale of the heart chambers and are typically no more than one wavelength away from a boundary. Thus the ‘snake instability’ may not be a problem in a real heart.

#### Acknowledgement

We are grateful to S. Alonso for helpful advice on details of simulations described in [7, 18]. This study was supported in part by EPSRC grant EP/D500338/1.

- 
- [1] P. K. Brazhnik, V. A. Davydov, V. S. Zykov, and A. S. Mikhailov, *JETP* **93**, 1725 (1987).
  - [2] V. N. Biktashev, A. V. Holden, and H. Zhang, *Phil. Trans. Roy. Soc. Lond. ser. A* **347**, 611 (1994).
  - [3] A. T. Winfree, *Science* **266**, 1003 (1994).
  - [4] V. N. Biktashev, *Int. J. of Bifurcation and Chaos* **8**, 677 (1998).
  - [5] F. Fenton and A. Karma, *Phys. Rev. Lett.* **81**, 481 (1998).
  - [6] F. Fenton and A. Karma, *Chaos* **8**, 20 (1998).
  - [7] S. Alonso, F. Sagues, and A. S. Mikhailov, *Science* **299**, 1722 (2003).
  - [8] S. Alonso, F. Sagues, and A. S. Mikhailov, *Journal of Physical Chemistry A* **110**, 12063 (2006).
  - [9] S. Alonso and A. V. Panfilov, *Chaos* **17**, 015102 (2007).
  - [10] R. Gray and J. Jalife, *Int. J. of Bifurcation and Chaos* **6**, 415 (1996).
  - [11] G. Boriani, M. Biffi, P. Silvestri, C. Martignani, C. Valzania, I. Diemberger, C. Moulder, G. Mouchawar, M. Kroll, and A. Branzi, *Heart Rhythm* **2**, 708 (2005).
  - [12] V. A. Davydov, V. S. Zykov, A. S. Mikhailov, and P. K. Brazhnik, *Radiofizika* **31**, 574 (1988).
  - [13] K. I. Agladze, V. A. Davydov, and A. S. Mikhailov, *JETP Lett.* **45(12)**, 767 (1987).
  - [14] V. N. Biktashev and A. V. Holden, *Phys. Lett. A* **181**, 216 (1993).
  - [15] V. N. Biktashev and A. V. Holden, *Chaos Solitons & Fractals* **5**, 575 (1995).
  - [16] V. N. Biktashev and A. V. Holden, *J. theor. Biol.* **169**, 101 (1994).
  - [17] A. V. Panfilov and A. N. Rudenko, *Physica D* **28**, 215 (1987).
  - [18] S. Alonso, F. Sagues, and A. S. Mikhailov, *Chaos* **16**, 023124 (2006).
  - [19] D. Barkley, *Physica D* **49**, 61 (1991).
  - [20] M. Dowle, R. M. Mantel, and D. Barkley, *Int. J. of Bifurcation and Chaos* **7**, 2529 (1997).
  - [21] A. V. Panfilov, A. N. Rudenko, and A. M. Pertsov, *Doklady akademii nauk SSSR* **279**, 1000 (1984).
  - [22] A. S. Mikhailov, A. V. Panfilov, and A. N. Rudenko, *Phys. Lett. A* **109**, 246 (1985).
  - [23] N. J. Wu, H. Zhang, H. P. Ying, Z. Cao, and G. Hu, *Phys. Rev. E* **73**, 060901(R) (2006).
  - [24] E. V. Nikolaev, V. N. Biktashev, and A. V. Holden, *Chaos Solitons and Fractals* **9**, 363 (1998).
  - [25] A. V. Panfilov, S. C. Müller, V. S. Zykov, and J. P. Keener, *Phys. Rev. E* **61**, 4644 (2000).
  - [26] V. S. Zykov and H. Engel, in *Analysis and Control*

*of Complex Nonlinear Processes in Physics, Chemistry and Biology*, edited by L. Schimansky-Geier, B. Fiedler, J. Kurths, and E. Schoell (World Scientific, Singapore, 2007).

[27] V. S. Zykov, O. U. Kheowan, O. Rangsiman, and S. C.

Müller, Phys. Rev. E. **65**, 026206 (2002).

[28] J. Schlesner, V. S. Zykov, H. Brandstadter, I. Gerdes, and H. Engel, New Journal of Physics **10** (2008).